ONE-DIMENSIONAL SEMI-COHERENT OPTICAL MODEL FOR THIN FILM SOLAR CELLS WITH ROUGH INTERFACES

Janez Krč, Franc Smole and Marko Topič

Faculty of Electrical Engineering, University of Ljubljana, Ljubljana, Slovenia

Key words: semiconductors, a-Si:H, Hydrogenated amorphous Silicon, thin-film solar cells, optical modelling, one-dimensional semi-coherent optical models, rough interfaces, smooth interfaces, light scattering, coherent light, scattered light, light absorption, QE, Quantum Efficiency, light trapping, TCO, Transparent Conductive Oxides, experimental results

Abstract: Optical model for thin film solar cells with rough interfaces is presented. In contrast to previous optical models, the presented model considers the coherent nature of direct (non-scattered) light, which is treated as electromagnetic waves, all over the structure. Therefore, the model accounts also for the interference pattern, which appears in the measured wavelength-dependent characteristics of the solar cells with rough interfaces. The model includes scattering of direct and already scattered incident light at all rough interfaces. In the paper, optical circumstances at flat and rough interfaces are described in detail. Coherent propagation of non-scattered and incoherent spreading of scattered light is defined and the calculation procedure in the model is addressed. The optical model is verified for a single junction hydrogenated amorphous silicon *p-i-n* solar cell deposited on Asahi U - type substrate. A good agreement, also in the interference pattern, verifies the applicability of the developed optical model.

Eno-dimenzionalni delno-koherentni optični model tankoplastnih sončnih celic s hrapavimi spoji

Ključne besede: polprevodniki, a-Si:H silicij amorfni hidrogeniziran, celice sončne tankoplastne, modeliranje optično, modeli optični delno-koherentni eno-dimenzionalni, ploskve mejne hrapave, ploskve mejne gladke, razprševanje svetlobe, svetloba koherentna, svetloba razpršena, vpijanje svetlobe, QE učinkovitost kvantna, ujetje svetlobe, TCO oksidi transparentni prevodni, rezultati eksperimentalni

Izvleček: Predstavljen je nov optični model tankoplastnih sončnih celic s hrapavimi spoji. Poglavitna prednost modela je, da upošteva koherentni značaj usmerjenega dela svetlobe, ki je obravnavan kot elektromagnetno valovanje preko celotne strukture. Zaradi tega model zajema tudi interferenčne pojave svetlobe v strukturi, katerih posledica so interferenčne oscilacije v valovno odvisnem kvantnem izkoristku sončne celice. Model vključuje tako razprševanje usmerjene kot tudi že razpršene vpadne svetlobe na hrapavih spojih. V članku so podrobno opisane optične razmere na gladkih in hrapavih spojih. Predstavljen je opis širjenja koherentne usmerjene in nekoherentne razpršene svetlobe. Naveden je potek izračuna svetlobne intenzitete v modelu po celotni strukturi sončne celice. Model je verificiran na podlagi izmerjenega poteka kvantnega izkoristka amorfnosilicijeve sončne celice, ki je bila izdelana na standardnemu "Asahi U" hrapavem substratu. Dobro ujemanje simulacije z meritvijo, tudi v poteku interferenčnih oscilacij, potrjuje uporabnost razvitega optičnega modela.

I. Introduction

To enhance light absorption in thin film solar cells, light trapping should be implemented in the multi-layer structure of the solar cell. One of the most commonly used light trapping technique is scattering of incident light at rough internal interfaces, which is usually introduced in the solar cell structure by using rough substrates. Multi-directional spreading of scattered light increases the effective path of light propagation in the thin layers resulting in higher absorption. Additionally, higher reflection of scattered light at internal interfaces, originating from non-perpendicular incidence of scattered light beams at the interfaces, assures more efficient light trapping in the solar cell.

The description of light scattering at rough interfaces in thin film solar cells presents a comprehensive problem, since the morphology of the interfaces is usually random and the root-mean-square roughness, σ_{rms}, of the interfaces is in the same order as the wavelength of incident light, λ. This complicates analytical description of the problem /1/. Additionally, the interference pattern, which can be observed in the wavelength-dependent characteristics of the solar cells (e.g. quantum efficiency, *QE*) indicates that besides the scattered light there still exists a significant amount of direct non-scattered light that propagates coherently throughout the structure.

To analyse and optimise the complex optical process an optical modelling is required. In the simulations an optical model that incorporates both, light scattering and coherent propagation of direct light, should be used. In order to describe the scattering process in the model, it has to be determined the amount of scattered light at each rough interface and how the light is scattered in reflection and in transmission at the interface. Previous publications /2-7/ indicated that the amount of scattered light at a rough interface can be approximately determined by means of scalar scattering theory /7-9/ which defines the ratio between diffused (scattered) and total (diffused + specular) amount of light. To describe how the light is scattered, an angular distribution function of scattered light, $f(\varphi)$, has to be determined.

Some one-dimensional optical models for thin-film solar cells with rough interfaces have already been developed /2-6/. In most of the models the direct light is not taken coherently, thus the simulated *QEs* can not reproduce the interference pattern observed in measurements. In this paper we present a new one-dimensional semi-coherent optical model that includes light scattering at all rough interfaces in the solar cell and considers the coherent propagation of direct light all over the structure. The optical situation at flat and rough interface is described in detail for direct and scattered light. In case of scattered light falling at a rough interface additional scattering in reflection and in transmission is taken into account. The analysis of coherent propagation of direct and incoherent spreading of scattered light is described. The model is verified with the measured *QE* of a thin film hydrogenated amorphous silicon (*a*-Si:H) *p-i-n* solar cell.

II. Optical model

In the developed one-dimensional semi-coherent optical model we assume perpendicular input illumination with direct coherent light (Fig. 1). All the interfaces in the multilayer structure are assumed to be parallel. This situation can be considered as a good approximation of usual circumstances in real thin film solar cells. Because of multiple reflections and transmissions at the interfaces, the direct light (dir) and scattered light (scatt), which is formed at rough interfaces (vertical arrows in the figure), is propagating in forward (+) and backward (-) direction. In the figure the direct light is presented by wavy arrows, indicating its coherent nature, whereas the dispersed nature of scattered light is shown by a sheaf of straight arrows. In case of direct light where forward-going and backward-going waves are represented by $I_{dir}^{+}(l,x)$ and $I_{dir}^{-}(l,x)$, there exists also an interference component $K(l,x)$, which has either forward or backward direction. The symbol l and x stands for wavelength- and position- dependency of the light intensities, respectively. The components of scattered light, $I_{scatt}^{+}(l,j,x)$ and $I_{scatt}^{-}(l,j,x)$, are also angular (j) dependent in order to indicate their directions of spreading. Since in numerical analysis the angle j is discretised, scattered light can be represented by a sheaf of light beams spreading in discrete directions j_i.

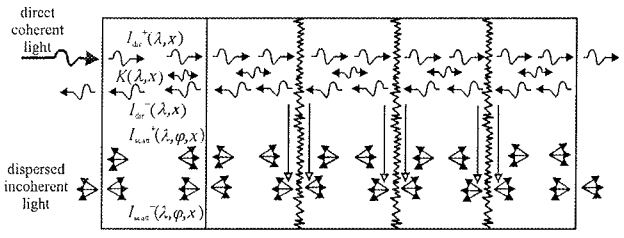

Fig. 1: Propagation of direct coherent light and spreading of scattered incoherent light in a thin film solar cell structure with smooth and rough interfaces.

The analysis of direct coherent light is based on the theory of electromagnetic waves. In general, the electromagnetic waves are presented by complex values of electric and magnetic field strengths distributed in the space. In the model all the waves of direct light are assumed to be planar and transversal (TEM) /10/, therefore they can be presented by electric field strengths $E^{+}(\lambda,x)$ and $E^{-}(\lambda,x)$ for forward-going and backward-going waves only. From $E^{+}(\lambda,x)$ and $E^{-}(\lambda,x)$ the individual components of direct light, $I_{dir}^{+}(\lambda,j,x)$, $I_{dir}^{-}(\lambda,j,x)$ and $K(\lambda,x)$, and the total intensity, $I_{dir}(\lambda,x) = I_{dir}^{+}(\lambda,j,x) - I_{dir}^{-}(\lambda,j,x) - K(\lambda,x)$, can be determined by Eq. 1. The symbols $n(\lambda)$ and $k(\lambda)$ present the real and the imaginary part of layer's complex refractive index $N(\lambda) = n(\lambda) - jk(\lambda)$. Y_0 is the optical admittance of free space ($Y_0 = 2.6544 \cdot 10^{-3}$ S). The superscript '*' denotes a conjugated complex number whereas "Im" stands for imaginary part of the complex number.

$$I_{dir}(\lambda,x) = \frac{1}{2} Y_0 \left[n(\lambda) \left| E^{+}(\lambda,x) \right|^2 - n(\lambda) \left| E^{-}(\lambda,x) \right|^2 - 2k(\lambda)\,\mathrm{Im}\left[E^{-}(\lambda,x) E^{+*}(\lambda,x) \right] \right]$$

$$= I_{dir}^{+}(\lambda,x) - I_{dir}^{-}(\lambda,x) - K(\lambda,x) \qquad (1)$$

The scattered light is analysed incoherently in the model, therefore it can be presented by the intensities $I_{scatt}^{+}(\lambda, \varphi, x)$ and $I_{scatt}^{-}(\lambda, \varphi, x)$ directly and not by electric field strengths of the electromagnetic waves.

In the model the optical circumstances at flat and rough interfaces are specified for direct coherent and scattered incoherent light. In sections II.A - II.D all four combinations (flat interface - direct light, flat interface - scattered light, rough interface - direct light and rough interface - scattered light) are described in detail. In section II.E the propagation of direct light and spreading of scattered light across the structure are determined. To simplify the indexing of light intensities, the subscripts "dir" and "scatt" are left out in further analysis. At the interfaces also positional dependency (x) is left out from the denotations of light intensities.

II.A Incidence of direct coherent light at a flat interface

Since the electromagnetic waves of direct light are transversal and since they propagate perpendicularly to the interfaces, all the components of electric field strengths are parallel to the interfaces, as depicted in Fig. 2.

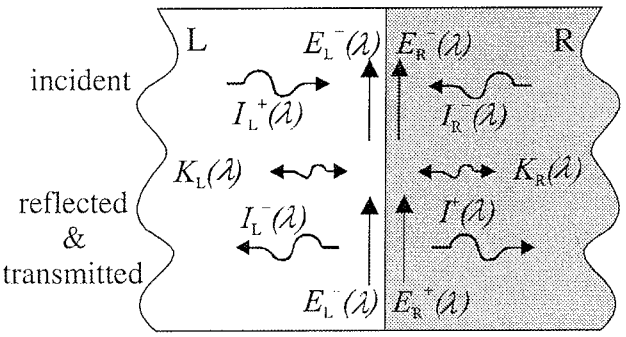

Fig. 2: *Electromagnetic waves of direct coherent light at a flat interface.*

Therefore, in the model the electric field strengths on the left (L) side, $E_L^+(\lambda)$ and $E_L^-(\lambda)$, can be calculated from the known values of electric field strengths on the right (R) side of the interface, $E_R^+(\lambda)$ and $E_R^-(\lambda)$, by Eq. 2 and Eq. 3, respectively. The symbols $N_L(\lambda)$ and $N_R(\lambda)$ correspond to complex refractive indexes of the left and right layer forming the interface.

$$E_L^+(\lambda) = \frac{1}{2}\left[\frac{N_L(\lambda)+N_R(\lambda)}{N_L(\lambda)} E_R^+(\lambda) + \frac{N_L(\lambda)-N_R(\lambda)}{N_L(\lambda)} E_R^-(\lambda)\right] \quad (2)$$

$$E_L^-(\lambda) = \frac{1}{2}\left[\frac{N_L(\lambda)-N_R(\lambda)}{N_L(\lambda)} E_R^+(\lambda) + \frac{N_L(\lambda)+N_R(\lambda)}{N_L(\lambda)} E_R^-(\lambda)\right] \quad (3)$$

In the figure $E_L^+(\lambda)$ and $E_R^-(\lambda)$ are the electric field strengths of the incident light which falls to the interface from left and right side, respectively, whereas $E_L^-(\lambda)$ and $E_R^+(\lambda)$ present the combined components of reflected and transmitted direct light. The corresponding light intensities at left side, $I_L^+(\lambda)$, $I_L^-(\lambda)$ and $K_L(\lambda)$, and right side, $I_R^+(\lambda)$, $I_R^-(\lambda)$ and $K_R(\lambda)$, of the interface can be calculated by means of Eq. 1.

II.B Incidence of scattered light at a flat interface

In Fig. 3, the situation at a flat interface illuminated with scattered light from left side, $I_L^+(\lambda, \varphi_L)$, and right side, $I_R^-(\lambda, \varphi_R)$, is symbolically illustrated. In this case the angular dependent intensities of reflected (r) light, $I_{Lr}^-(\lambda, \varphi_{Lr})$ and $I_{Rr}^+(\lambda, \varphi_{Rr})$, and transmitted (t) ligh $I_{Lt}^-(\lambda, \varphi_{Lt})$ and $I_{Rt}^+(\lambda, \varphi_{Rt})$, are shown separately in the figure. At the interface, for each discrete beam of incident light the intensity and direction (angle) of reflected and transmitted components has to be determined. Due to superposition of the intensities, which can be assumed for incoherent scattered light, the situation can be analysed for left and right side illumination independently. Next we focus on left side illumination only.

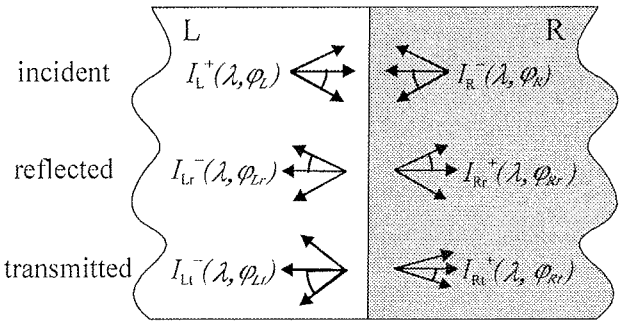

Fig. 3: *Intensities of scattered light at a flat interface.*

If the intensity of the left side illumination, $I_L^+(\lambda,\varphi_L)$, is known the reflected, $I_{Lr}^-(\lambda,\varphi_{Lr})$, and transmitted, $I_{Rt}^+(\lambda,\varphi_{Rt})$, components can be calculated by Eq. 4 and Eq. 5, respectively. The angles φ_L, φ_{Lr} and φ_{Rt} correspond to the directions of incident, reflected and transmitted light beams, respectively. The $R_{HV\,L}(\lambda,\varphi_L, \varphi_{Rt})$ and $T_{HV\,Lr}(\lambda,\varphi_L, \varphi_{Rt})$ are reflectance and transmittance at a flat interface and will be explained in following.

$$I_{Lr}^-(\lambda,\varphi_{Lr}) = R_{HV\,L}(\lambda,\varphi_L,\varphi_{Rt})\cdot I_L^+(\lambda,\varphi_L) \quad (4)$$

$$I_{Rt}^+(\lambda,\varphi_{Rt}) = T_{HV\,Lr}(\lambda,\varphi_L,\varphi_{Rt})\cdot I_L^+(\lambda,\varphi_L) \quad (5)$$

Since the light beams of scattered light do not fall perpendicularly on the interface, in general the reflectance and transmittance should be defined for horizontally, (H) and vertically, (V) polarized light /10/. The reflectance of horizontal polarisation, $R_{H\,L}(\lambda,\varphi_L, \varphi_{Rt})$, and vertical polarisation, $R_{V\,L}(\lambda,\varphi_L, \varphi_{Rt})$, are defined by Eq. 6 and Eq. 7, respectively,

$$R_{H\,L}(\lambda,\varphi_L,\varphi_{Rt}) = \left|\frac{N_L(\lambda)\cdot\cos\varphi_L - N_R(\lambda)\cdot\cos\varphi_{Rt}}{N_L(\lambda)\cdot\cos\varphi_L + N_R(\lambda)\cdot\cos\varphi_{Rt}}\right|^2 \quad (6)$$

$$R_{V\,L}(\lambda,\varphi_L,\varphi_{Rt}) = \left|\frac{N_L(\lambda)\cdot\cos\varphi_{Rt} - N_R(\lambda)\cdot\cos\varphi_L}{N_L(\lambda)\cdot\cos\varphi_{Rt} + N_R(\lambda)\cdot\cos\varphi_L}\right|^2 \quad (7)$$

Since the light polarisation in the multi-layer structures with rough interfaces can not be exactly determined, we use in the model an average reflectance $R_{HV\,L}(\lambda,\varphi_L, \varphi_{Rt})$, which was chosen as a mean value of $R_{H\,L}(\lambda,\varphi_L, \varphi_{Rt})$ and $R_{V\,L}(\lambda,\varphi_L, \varphi_{Rt})$. The corresponding average transmittance $T_{HV\,LR}(\lambda,\varphi_L, \varphi_{Rt})$ for the scattered light beams is simply calculated from the $R_{HV\,L}(\lambda,\varphi_L, \varphi_{Rt})$ using Eq. 8.

$$T_{HV\,LR}(\lambda,\varphi_L,\varphi_{Rt}) = 1 - R_{HV\,L}(\lambda,\varphi_L,\varphi_{Rt}) \quad (8)$$

By means of $R_{HVL}(\lambda, \varphi_L, \varphi_{Rt})$ and $T_{HVLR}(\lambda, \varphi_L, \varphi_{Rt})$ the amount of reflected and transmitted light can be determined. To define the directions (angles) of the reflected and transmitted beams the Fresnell refractive law is used /10/. Thus, the angle in reflection, φ_{Lr}, is determined as a negative value of the corresponding incident angle, φ_L, whereas the angle in transmission, φ_{Rt}, is calculated using Eq. 9 where $n_L(\lambda)$ and $n_R(\lambda)$ are the real parts of refractive indexes of the layers forming the interface.

$$\varphi_{Rt} = \arcsin\left(\frac{n_L(\lambda)}{n_R(\lambda)} \sin \varphi_L\right) \tag{9}$$

II.C Incidence of direct light at a rough interface

At a rough interface the amount of scattered light and its angular distribution function have to be determined. The scalar scattering theory can be used as an approximation to define the amount of scattered (diffused) and non-scattered (specular) light in reflection and in transmission. If the direct incident light were taken incoherently and the illumination were applied from left side of the interface only, the specular and diffused parts of light could be determined by specular and diffuse reflectances, $R_{Lspec}(\lambda)$ (Eq. 10) and $R_{Ldif}(\lambda)$ (Eq. 11), and specular and diffused transmittances, $T_{LRspec}(\lambda)$ (Eq. 12) and $T_{LRdif}(\lambda)$ (Eq. 13).

$$R_{Lspec}(\lambda) = R_0(\lambda) \cdot e^{-\left(\frac{4\pi\sigma_{rms} c_r n_L(\lambda)}{\lambda}\right)^2} \tag{10}$$

$$R_{L\,dif}(\lambda) = R_0(\lambda) - R_{Lspec}(\lambda) \tag{11}$$

$$T_{LRspec}(\lambda) = T_0(\lambda) \cdot e^{-\left(\frac{4\pi\sigma_{rms} c_t |n_L(\lambda) - n_R(\lambda)|}{\lambda}\right)^3} \tag{12}$$

$$T_{LRdif}(\lambda) = T_0(\lambda) - T_{LRspec}(\lambda) \tag{13}$$

The parameters c_r (Eq. 10) and c_t (Eq. 12) are the correction factors for specular reflectance and transmittance which can vary between 0 and 1 /7/. $R_0(\lambda)$ and $T_0(\lambda)$ are total (specular + diffused) reflectance and transmitance which are assumed to be the same as in the case of a flat interface and can be defined by Eq. 14 and Eq. 15, respectively

$$R_0(\lambda) = \left|\frac{N_L(\lambda) - N_R(\lambda)}{N_L(\lambda) + N_R(\lambda)}\right|^2 \tag{14}$$

$$T_0(\lambda) = 1 - R_0(\lambda) \tag{15}$$

In the model, the direct light is treated coherently, but the Eqs. 10-15 are still assumed to be valid for the light intensities. In the case it is necessary to start the analysis on electric field strengths of the specular components. Further explanation will be based on Fig. 4, where a rough interface is illuminated with direct coherent light from both sides, as in the case of flat interface in Sec. II.A.

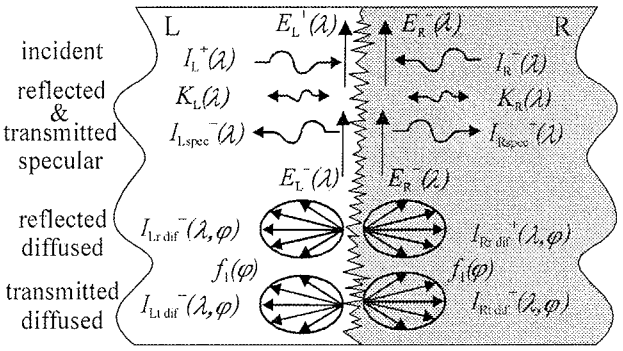

Fig. 4: *Incidence of direct coherent light at a rough interface.*

At the rough interface, the electric field strengths of coherent light on the right side, $E_R^+(\lambda)$ and $E_R^-(\lambda)$, are firstly transformed to the corresponding intensities $I_{Rspec}^+(\lambda)$, $I_R^-(\lambda)$ and $K_R(\lambda)$ using Eq. 1. Then, the value of $K_R(\lambda)$ is added either to $I_{Rspec}^+(\lambda)$ or to $I_R^-(\lambda)$, according to its direction (sign), resulting in two components, $I_{RK}^+(\lambda)$ and $I_{RK}^-(\lambda)$ defined by Eq. 16 and Eq. 17, respectively.

$$I_{RK}^+(\lambda) = \begin{cases} I_{R\,spec}^+(\lambda) - K_R(\lambda) \; ; \; K_R(\lambda) < 0 \\ I_{R\,spec}^+(\lambda) \quad\quad\quad\quad ; \; K_R(\lambda) \geq 0 \end{cases} \tag{16}$$

$$I_{RK}^-(\lambda) = \begin{cases} I_R^-(\lambda) \quad\quad\quad\quad ; \; K_R(\lambda) < 0 \\ I_R^-(\lambda) + K_R(\lambda) \; ; \; K_R(\lambda) \geq 0 \end{cases} \tag{17}$$

From $I_{RK}^+(\lambda)$ and $I_{RK}^-(\lambda)$ the components $I_{LK}^+(\lambda)$ and $I_{LK}^-(\lambda)$ of specular light on the left side of the interface can be determined, using Eq. 18 and Eq. 19, respectively.

$$I_{LK}^+(\lambda) = \frac{1}{T_{LR\,spec}(\lambda)} \cdot I_{RK}^+(\lambda) - \frac{R_{R\,spec}(\lambda)}{T_{LR\,spec}(\lambda)} \cdot I_{RK}^-(\lambda) \tag{18}$$

$$I_{LK}^-(\lambda) = \frac{R_{L\,spec}(\lambda)}{T_{LR\,spec}(\lambda)} \cdot I_{RK}^+(\lambda) - \frac{R_{R\,spec}(\lambda) \cdot R_{L\,spec}(\lambda) - T_{RL\,spec}(\lambda) T_{LR\,spec}(\lambda)}{T_{LR\,spec}(\lambda)} \cdot I_{RK}^-(\lambda) \tag{19}$$

In the equations the reflectance $R_{R\,spec}(\lambda)$ and transmittance $T_{RL\,spec}(\lambda)$ correspond to the case of right side illumination. They can be determined by Eq. 10 and Eq. 12 where all indexes "L" should be substituted with "R" and vice versa.

From the calculated intensities $I_{L\,K}^{+}(\lambda)$ and $I_{L\,K}^{-}(\lambda)$ the absolute values of electric field strengths of coherent light, $|E_L^{+}(\lambda)|$ and $|E_L^{-}(\lambda)|$, on the left side can be obtained if the direction (sign) of $K_L(\lambda)$ is known. The sign of $K_L(\lambda)$ can be determined if the phases, $J_L^{+}(\lambda)$ and $J_L^{-}(\lambda)$, of the electric field strengths ($E_L^{+}(\lambda)=|E_L^{+}(\lambda)|e^{j\vartheta L+(\lambda)}$ and $E_L^{-}(\lambda)=|E_L^{-}(\lambda)|e^{j\vartheta L-(\lambda)}$) are known. Simulations indicated that these phases have significant influence on the position of the interference pattern in the wavelength dependent *QE* of the solar cells. Moreover, from measured *QEs* of the solar cells can be observed that the position of the interference pattern is in general not affected by the σ_{rms}. The value of the σ_{rms} influences only the intensity of the interference pattern. These findings lead us to the assumption that in case of a rough interface the phases of electric field strengths can be deduced from the case of flat interface. Thus, to determine $\vartheta_L^{+}(\lambda)$ and $\vartheta_L^{-}(\lambda)$, first the electric field strengths, $E_L'^{+}(\lambda)$ and $E_L'^{-}(\lambda)$, of the corresponding flat interface are calculated by means of Eq. 2 and Eq. 3. Then, the phases $\vartheta_L^{+}(\lambda)=\vartheta_L'^{+}(\lambda)$ and $\vartheta_L^{-}(\lambda)=\vartheta_L'^{-}(\lambda)$ can be determined by Eq. 20 where "+" and "-" signs correspond to the electric field strength of forward-going and backward-going waves, respectively.

$$\vartheta_L^{+/-}(\lambda)=\begin{cases}\operatorname{arctg}\left(\dfrac{\operatorname{Im}\left[E_L'^{+/-}(\lambda)\right]}{\operatorname{Re}\left[E_L'^{+/-}(\lambda)\right]}\right) & ;\ \operatorname{Re}\left[E_L'^{+/-}(\lambda)\right]\geq 0\\ \operatorname{arctg}\left(\dfrac{\operatorname{Im}\left[E_L'^{+/-}(\lambda)\right]}{\operatorname{Re}\left[E_L'^{+/-}(\lambda)\right]}\right)+\pi & ;\ \operatorname{Re}\left[E_L'^{+/-}(\lambda)\right]<0\end{cases} \tag{20}$$

From the relation $K_L(\lambda) = Y_0 k(\lambda)\operatorname{Im}[E^{-}(\lambda)\,E^{+*}(\lambda)]$, which originates from Eq. 1, it can be found out that the sign of $K_L(\lambda)$ can be indicated by Eq. 21.

$$\begin{aligned}\sin(\vartheta_L^{-}(\lambda)-\vartheta_L^{+}(\lambda))>0 \Rightarrow\ & K_L(\lambda)>0\\ else\qquad\qquad\quad & K_L(\lambda)\leq 0\end{aligned} \tag{21}$$

In further analysis we use Eqs. 16-17 and substituting index "R" with index "L", since the left side of the interface is under scope. According to the sign of $K_L(\lambda)$ appropriate relations for $I_{L\,K}^{+}(\lambda)$ and $I_{L\,K}^{-}(\lambda)$ can be chosen from Eqs. 16-17. Based on Eq. 1, $I_{Lspec}^{+}(\lambda)$, $I_{Lspec}^{-}(\lambda)$ and $K_L(\lambda)$ can be written in terms of $E_L^{+}(\lambda)$ and $E_L^{-}(\lambda)$, where $E_L^{+}(\lambda)$ and $E_L^{-}(\lambda)$ can be represented by their absolute values and phases. Since the phases are already known the two absolute values of electric field strengths, $|E_L^{+}(\lambda)|$ and $|E_L^{-}(\lambda)|$, can be easily obtained. In the case of negative $K_L(\lambda)$ the $|E_L^{-}(\lambda)|$ is determined by Eq. 22 whereas the $|E_L^{+}(\lambda)|$ is implicitly given by Eq. 23.

$$\left|E_L^{-}(\lambda)\right|=\sqrt{\frac{2\cdot I_{L\,K}^{-}(\lambda)}{Y_0 n_L(\lambda)}} \tag{22}$$

$$\frac{1}{2}Y_0 n_L(\lambda)\cdot\left|E_L^{+}(\lambda)\right|^2-Y_0 k_L(\lambda)\cdot\left|E_L^{-}(\lambda)\right|\cdot\sin(\vartheta_L^{-}(\lambda)-\vartheta_L^{+}(\lambda))\cdot\left|E_L^{+}(\lambda)\right|-I_{L\,K}^{+}(\lambda)=0 \tag{23}$$

If $K_L(\lambda)$ is positive, the role of $|E_L^{-}(\lambda)|$ and $|E_L^{+}(\lambda)|$ in Eq. 22-23 exchanges.

Knowing $|E_L^{-}(\lambda)|$, $|E_L^{+}(\lambda)|$, $J_L^{+}(\lambda)$ and $J_L^{-}(\lambda)$, the complex electric field strengths of the specular coherent light on the left side of the rough interface are determined and the corresponding specular intensities $I_{Lspec}^{+}(\lambda)$, $I_{Lspec}^{-}(\lambda)$ and $K_L(\lambda)$ can be calculated.

The diffused components in reflection, $I_{Lr\,dif}^{-}(\lambda,\varphi)$, $I_{Rr\,dif}^{+}(\lambda,\varphi)$, and in transmission, $I_{Lt\,dif}^{-}(\lambda,\varphi)$, $I_{Rt\,dif}^{+}(\lambda,\varphi)$, can be calculated from $I_{L\,K}^{+}(\lambda)$ and $I_{R\,K}^{-}(\lambda)$ which presents the illumination from left and right side of the interface, respectively. By determining the incoherent diffused parts of light, the superposition of left and right side illumination is assumed. Therefore, we will determine only the components $I_{Lr\,dif}^{-}(\lambda,\varphi)$, and $I_{Rt\,dif}^{+}(\lambda,\varphi)$ which correspond to the left side illumination. The diffused component in reflection, $I_{Lr\,dif}^{-}(\lambda,\varphi)$, and in transmission, $I_{Rt\,dif}^{+}(\lambda,\varphi)$, can be calculated by Eqs. 24-25. $R_{L\,dif}(\lambda)$ and $T_{LR\,dif}(\lambda)$ were defined by Eq. 11 and Eq. 13, respectively. The angular distribution function for the case of direct incident light, $f_1(\varphi)$, was chosen to be a normalised $\cos^2(\varphi)$ function /7/ in our simulations. However, $f(\varphi)$ is an input parameter of our optical model, thus an arbitrary selection of $f(\varphi)$ can be made.

$$I_{Lr\,dif}^{-}(\lambda,\varphi)=f(\varphi)\cdot R_{L\,dif}(\lambda)\cdot I_{L\,K}^{+}(\lambda) \tag{24}$$

$$I_{Rt\,dif}^{+}(\lambda,\varphi)=f(\varphi)\cdot T_{LR\,dif}(\lambda)\cdot I_{L\,K}^{+}(\lambda) \tag{25}$$

II.D Incidence of scattered light at a rough interface

For scattered incident light it is assumed that a part of it is additionally dispersed at a rough interface (diffused part) while the rest is spread as in the case of flat interface (specular part). A general situation, where the scattered light falls on a rough interface from left and right side is symbolically illustrated in Fig. 5.

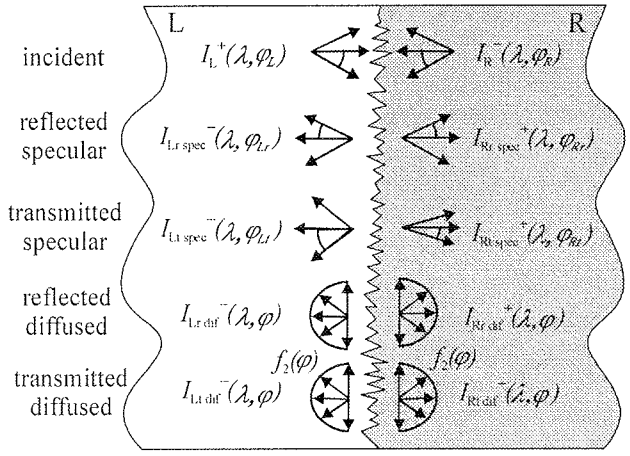

Fig. 5: Incidence of scattered incoherent light at a rough interface.

Due to the superposition we describe the analysis for the case of left side illumination only. To determine specular reflectance and transmittance for the case of scattered incident light, we have to introduce the angular dependency on the angle of incident light, φ_L, and the angles of transmitted light, φ_{Rt}, as shown in Eq. 26-27.

$$R_{Lspec}(\lambda,\varphi_L,\varphi_{Rt}) = R_{HV\,L}(\lambda,\varphi_L,\varphi_{Rt}) \cdot e^{-(\frac{4\pi\sigma_{rms}c_t n_L(\lambda)\cos\varphi_L}{\lambda})^2} \tag{26}$$

$$T_{LRspec}(\lambda,\varphi_L,\varphi_{Rt}) = T_{HV\,LR}(\lambda,\varphi_L,\varphi_{Rt}) \cdot e^{-(\frac{4\pi\sigma_{rms}c_t\,|n_L(\lambda)\cos\varphi_L - n_R(\lambda)\cos\varphi_{Rt}|}{\lambda})^3} \tag{27}$$

For diffused reflectance and transmittance, which depend on angular distribution functions of incident scattered light $f_{inc}(\varphi)$ in our model, the average values $\overline{R}_{L\,dif}(\lambda)$ and $\overline{T}_{LR\,dif}(\lambda)$ defined by Eq. 28-29 are used

$$\overline{R}_{L\,dif}(\lambda) = \sum_i f_{inc}(\varphi_i)\cdot\left[R_{HV\,L\,spec}(\lambda,\varphi_i) - R_{L\,spec}(\lambda,\varphi_i)\right] \tag{28}$$

$$\overline{T}_{L\,dif}(\lambda) = \sum_i f_{inc}(\varphi_i)\cdot\left[T_{HV\,LR\,spec}(\lambda,\varphi_i) - T_{LR\,spec}(\lambda,\varphi_i)\right] \tag{29}$$

The angular distribution function of reflected and transmitted diffused light for scattered incident light, $f_2(\varphi)$, is expected to be broader than $f_{inc}(\varphi)$ since additional scattering at a rough interface takes place. In our model, we assume equal scattering in all directions resulting in half-circular $f_2(\varphi)$, in reflection and transmission, as shown in Fig. 5.

II.E Propagation of direct and scattered light

For direct coherent light, the propagation of forward-going and backward-going waves is defined on basis of electric field strengths as given by Eq. 30. The symbol x_0 presents the starting point of propagation whereas the $N(\lambda)$ is the complex refractive index of the layer in which the waves are propagated. The superscripts (+/-) stand for forward-going/backward-going waves of direct light.

$$E^{+/-}(\lambda,x) = E^{+/-}(\lambda,x_0)\,e^{-/+\frac{2\pi N(\lambda)}{\lambda}(x-x_0)} \tag{30}$$

The spreading of scattered light is in general a three-dimensional problem. Assuming the conical symmetry of light scattering in the real solar cells we can describe the spreading in one-dimensional model as follows. For a discrete beam of scattered light, which is propagating in the direction φ_i, we can determine the effective path of propagation given by $(x\text{-}x_0)/\cos\varphi_i$, as shown in Fig. 6.

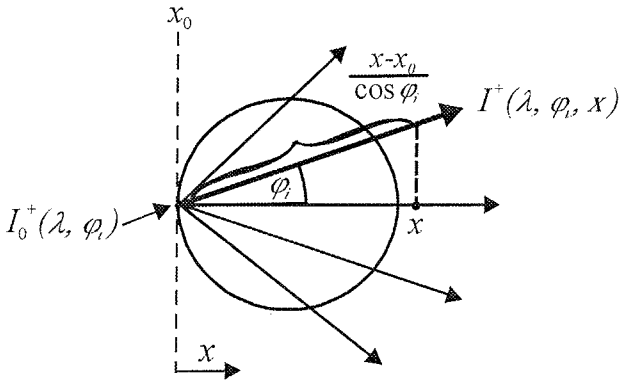

Fig. 6: Spreading of scattered light.

Considering the effective path, the propagation of the incoherent beam is defined by Eq. 31, where $\alpha(\lambda)$ presents the absorption coefficient of the layer. The superscripts denote forward direction (left side of the slash) and backward direction (right side of the slash) of the beam.

$$I^{+/-}(\lambda,\varphi_i,x) = I^{+/-}(\lambda,\varphi_i)\cdot e^{-/+\frac{\alpha(\lambda)}{\cos\varphi_i}\cdot(x-x_0)} \tag{31}$$

In the equation, the factor $1/\cos\varphi_i$ is applied to $\alpha(\lambda)$, which can be interpreted as the propagation in the perpendicular direction ($\varphi = 0$), but in the layer with enhanced absorption coefficient by factor $1/\cos\varphi_i$. By this method the propagation of all scattered beams can be determined in the model.

III. Calculation procedure in the model

For each monochromatic component λ of illumination spectrum the distribution of direct coherent light throughout the entire structure is calculated first. The calculation starts at the back (most right) side of the structure, where only for-

ward-going wave is present, since the solar cell is illuminated from front (most left) side only. In the same step of simulation, the diffused parts of direct incident light at each rough interface are determined. Further spreading of the scattered light is calculated iteratively by iterative two-step procedure. In the first step, only the propagation of forward-going components of scattered light is determined. In the second step, the same calculation is performed for backward-going scattered light. The steps are then repeated iteratively. Because of light absorption in the layers and transmittances through the interfaces, the intensities of scattered light are decreasing by iterating the calculation. The iterative procedure is terminated, when the last contribution of scattered light is reasonably small, comparing to the sum of contributions from previous iterations. After the light distribution of entire spectrum is determined, the final results of optical simulations - wavelength-dependent reflectances, absorptances in the individual layers and carrier generation profiles in the active layers - can be calculated.

IV. Verification of the model

With the developed optical model, we carried out the simulation of a single junction *a*-Si:H PIN solar cell structure deposited on standard Asahi U - type substrate, consisting of glass and rough Transparent Conductive Oxide (TCO) layer. The σ_{rms} of the TCO surface was measured to be 40 nm. A schematic view of the superstrate structure of the analysed solar cells and the thicknesses of individual layers are given in Fig. 7.

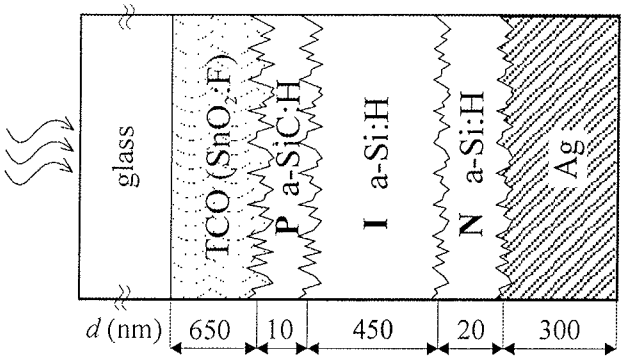

Fig. 7: *A schematic view of a-Si:H solar cell structure with rough interfaces.*

Since the deposited *a*-Si:H layers are relatively thin comparing the roughness of the TCO layer, all the subsequent layers of the structure are rough and have almost the same σ_{rms} as glass/TCO substrate.

The measured (symbols) and simulated (lines) *QE(λ)* of the solar cell are given in Fig. 8. The experimental data of the *QE* and the value of the σ_{rms} of the TCO surface were provided by Delft University of Technology /7/. The curve in Fig. 8 corresponds to the simulation with the developed semi-coherent optical model. In calculations of the *QE(λ)*, a simplified but justified electrical analysis was applied, assuming the ideal extraction of charge carriers from the active *i*-layer and neglecting the contribution of the *p*- and *n*-layer /7/. In the model, the $\cos^2\varphi$ function was used for the angular distribution function of the diffuse light in case of direct incident light, while in the case of scattered incident light the diffused light had half-circular distribution function.

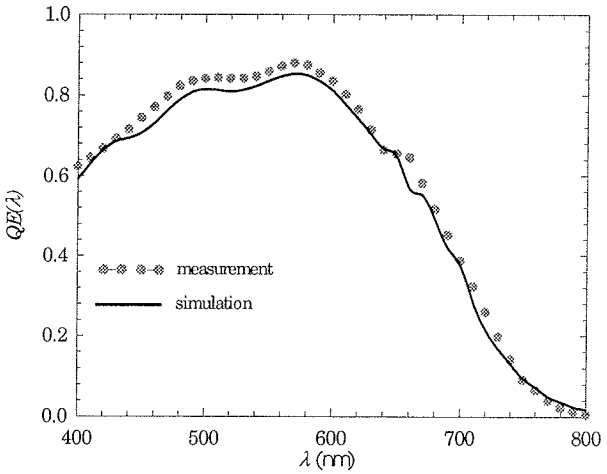

Fig. 8: *Measured (symbols) and simulated (lines) quantum efficiency of the a-Si:H solar cell.*

Fig. 8 reveals a good agreement between experimental data and simulation. In particular, the position and intensity of the interference pattern, which could not be obtained with previous incoherent optical models, is matched well with the measured one. The fringes of the pattern are only moderately pronounced in the case of analysed solar cell, since the roughness of standard Asahi U -type substrate is relatively high. We expect that further verification on samples with lower interface roughness, which exhibit enhanced interference fringes in the *QE(λ)*, will reveal the benefits of semi-coherent model even more evidently.

V. Conclusions

One-dimensional semi-coherent optical model for thin-film solar cells with rough interfaces was presented. In contrast to existing incoherent optical models, the direct (non-scattered) part of light is taken coherently all over the structure in our model. Thus, the simulations account also for the interference effects of direct light leading to the interference pattern in *QE*. Optical circumstances for direct coherent and scattered incoherent light at flat and rough interfaces were described and propagation of both types of light defined. At rough interfaces the scalar scattering theory was used in order to determine the specular and diffused part of light in reflection and in transmission. A preliminary verification of the model using a single junction *a*-Si:H solar cell with rough interfaces was carried out. A good agreement with experimental *QE* was obtained, indicating the applicability of the semi-coherent optical model.

Acknowledgement

The authors are very grateful to M. Zeman from DIMES, Delft University of Technology, for the experimental data and useful discussions.

References

/1/ J. J. Wallinga, *"Textured transparent electrodes and series integration for amorphou silicon solar cells"*, Doctoral Dissertation, Utrecht University, The Netherlands, 1998.

/2/ G. Tao, *"Optical modeling and Characterization of Hydrogenated Amorphous Silicon Solar Cells"*, Doctoral Dissertation, Delft University Press, The Netherlands, 1994.

/3/ F. Leblanc, J. Perrin, J. Schmitt, *"Numerical Modeling of the Optical Properties of Amorphous Silicon Based PIN Solar Cells Deposited on Rough Transparent Conducting Oxide Substrates"*, J. of Appl. Phys. 75, (2), pp. 1074-1087, 1994.

/4/ G. Tao, M. Zeman, J. W. Metselaar, *"Accurate Generation Rate Profiles in a-Si:H Solar Cells with Textured TCO Substrates"*, Sol. Energ. Mat. Sol. C., 34: (1-4), pp. 359-366, 1994.

/5/ A. Poruba, A. Fejfar, Z. Remeš, J. Špringer, M. Vaneček, J. Kočka, *"Optical absorption and light scattering in microcrystalline silicon thin films and solar cells"*, Journal of Applied Physics, Vol. 88, (2000), pp. 148-160.

/6/ J. Krč, M. Topič, M. Vukadinović, F. Smole, *"Optical Simulation of a-Si:H-Based PIN Solar Cell with Rough Back and Front TCO Layer"*, 36th MIDEM Conference Proc., pp. 253-258, Slovenia, 2000.

/7/ M. Zeman, R.A.C.M.M. van Swaaij, J.W. Metselaar, "Optical modelling of a-Si:H solar cells with rough interfaces: Effect of back contact and interface roughness", Journal of Applied Physics, Vol. 88, (2000), pp. 6436-6443.

/8/ H. E. Bennett, J. O. Porteus, *"Relation between surface roughness and specular reflectance at normal incidence"*, J. Opt. Soc. Am. Vol 51, 1961.

/9/ P. Beckmann, A. Spizzichino, *"The Scattering of Electromagnetic Waves from Rough Surfaces"*, Pergamon press, 1963.

/10/ Jin Au Kong, *"Electromagnetic wave theory"*, John Wiley&Sons, 1990.

Asst. Janez Krč, M. Sc.
Faculty of Electrical Engineering
University of Ljubljana
Tržaška 25, SI-1000 Ljubljana, SLOVENIA
tel.: +386 (0)1 4768 321, fax: +386 (0)1 4264 630
e-mail: janez.krc@fe.uni-lj.si

Prof. Dr. Franc Smole
Faculty of Electrical Engineering
University of Ljubljana
Tržaška 25, SI-1000 Ljubljana, SLOVENIA
tel.: 386 (0)1 4768 330, fax: 386 (0)1 4264 630
e-mail: franc.smole@fe.uni-lj.si

Assoc. Prof. Dr. Marko Topič
Faculty of Electrical Engineering
University of Ljubljana
Tržaška 25, SI-1000 Ljubljana, SLOVENIA
tel.: +386 (0)1 4768 470, fax: 386 (0)1 4264 630
e-mail: marko.topic@fe.uni-lj.si

Prispelo (Arrived): 5.1.2002 *Sprejeto (Accepted): 26.2.2002*